Design of guided mode resonant filters for authentication applications through azimuthal angles varying

Dawei Zhang (张大伟)[1], Limeng Yuan (袁丽萌)[1], Jiabi Chen (陈家璧)[1], Songlin Zhuang (庄松林)[1], and Hongbo He (贺洪波)[2]

[1] *College of Optics and Electronics, University of Shanghai for Science and Technology, Shanghai 200093*

[2] *Shanghai Institute of Optics and Fine Mechanics, Chinese Academy of Sciences, Shanghai 201800*

Received June 3, 2008

Guided mode resonant filters (GMRFs) for authentication application with low sideband reflection at 0° and 90° azimuthal angles were designed. Using rigorous coupled-wave analysis, the diffractive characteristics of this kind device with different illumination angles, groove depths, and thicknesses of cover SiO_2 layer were investigated. The structure of GMRF which satisfies the requirements for authentication applications was obtained. Illuminated at 30° for a definite polarization mode, the filter presents symmetrical reflectance shape, low sideband reflectance, two separate reflectance peaks, and definite full-width at half-maximum (FWHM) at 0° and 90° azimuthal angles.

OCIS codes: 050.0050, 090.0090, 230.0230.

doi: 10.3788/COL20080610.0776.

The guided mode resonant filter (GMRF) has two important features, narrow spectral response which was widely investigated[1−9] and variable optical effect which has not been so widely studied. The application of variable optical effect was first proposed by Gale *et al.*[10]. When the microstructures proposed by Gale are viewed at an angle and rotated, they show a distinctive color change from red to green, so the devices can be applied in the field of visual and machine readable security features. M. T. Gale did not design this kind of device from the GMRF point of view. Authentication labels with GMRF point of view were first reported in 2007 by Mount-Learn Wu and its variable optical effect was obtained through varying incidence angles[11].

The purpose of this work is to design good structures for an authenticating device based on GMRF through azimuthal angles varying. Using the rigorous coupled-wave analysis techniques[6], the optimum illumination angle is discussed first. At 30° illumination angle, the spectral responses of the authenticating device at 0° and 90° azimuthal angles are both successfully controlled at the same time. The reflection sideband of the GMRF is suppressed by a low refractive index cover layer. As a result, one good structure of a GMRF for authentication applications is obtained.

A device for authentication applications reported has a high index grating embedded in a low index medium with a period smaller than 400 nm. The construction details are shown in Fig. 1, and the geometry of the grating diffraction is shown in Fig. 2. The parameters Λ and f are the period and the fill factors of the grating respectively. To limit the scope of the present analysis, only the TE polarization mode at 0° azimuthal angle was considered in this work (at 90° azimuthal angle, the wave was regarded as TM polarization mode).

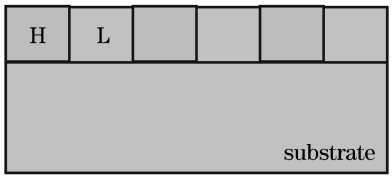

Fig. 1. Structure of single-layer GMRF. $n_{gH} = 2.35$, $n_{gL} = 1.46$, $n_{sub} = 1.46$, $\Lambda = 400$ nm, $f = 0.5$.

The illumination angle for authentication applications has not been detailed, however, it has an important effect on the reflectance response. The values of zero-order reflectance were calculated at different illumination angles. It can be found from Fig. 3(a) that for 0° azimuthal angle, the resonant wavelengths of GMRF are 44, 470, and 500 nm, corresponding to illumination angles of 30°, 50°, and 70°, respectively. Figure 3(b) shows that for 90° azimuthal angle, the resonant wavelengths of GMRF are 582, 540, and 501 nm corresponding to 30°, 50°, and 70° illumination angles, respectively. It can be observed that, when illumination angles increased from 30° to 70° and for 0° azimuthal angle, the resonant wavelength shifted to a long wavelength gradually. On the contrary, for 90° azimuthal angle, it shifted to a short wavelength. This kind of shift will weaken the spectral shift effect. In fact, when the illumination angle is 70°, as shown in Fig. 3, the values of the resonant wavelengths overlap at 0° and 90°

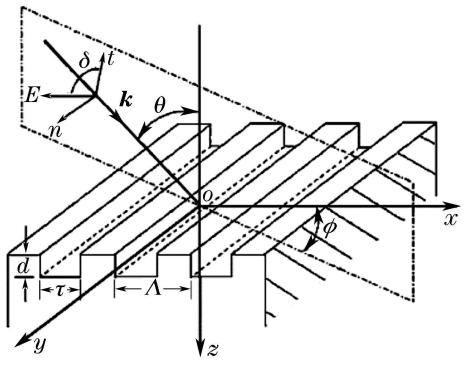

Fig. 2. Geometry for the grating diffraction problem analyzed herein. θ: illumination angle; ϕ: azimuthal angle; d: groove depth.

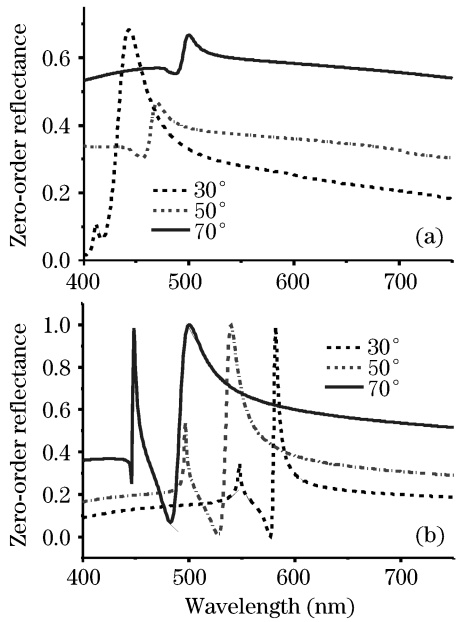

Fig. 3. Reflectance of GMRF for incident waves at 30°, 50°, and 70° illumination angles. $n_{\rm gH} = 2.35$, $n_{\rm gL} = 1.46$; $d = 80$ nm; $n_{\rm sub} = 1.46$; $\Lambda = 400$ nm; $f = 0.5$. (a) $\phi = 0°$; (b) $\phi = 90°$.

azimuthal angles. So the spectral shift effect will vanish at 70° illumination angle during the rotating of GMRF in plane. Furthermore, it can be found from Fig. 3(b) that with the increasing of illumination angle, the other reflectance peaks appear or increase. These peaks have bad effects on the spectral shift effect. To avoid this kind of bad effect, 30° is chosen as the illumination angle for the following calculation.

To enhance the spectral shift effect, the maximization of the main zero-order reflectance peak is needed. The dependence of two main peaks at 0° and 90° azimuthal angles on groove depth is given by Fig. 4. From it, we can find that when groove depth is 75 nm, the reflectance achieved its maximum nearly at 0° and 90° azimuthal angles. To investigate the spectral shift effect with this groove depth, the reflectance of GMRF with 0° and 9° azimuthal angles was calculated. As illustrated in Fig. 5, the main peak changes from 444 to 576 nm during the rotating of GMRF in plane. This result satisfies the requirement of optically variable authentication

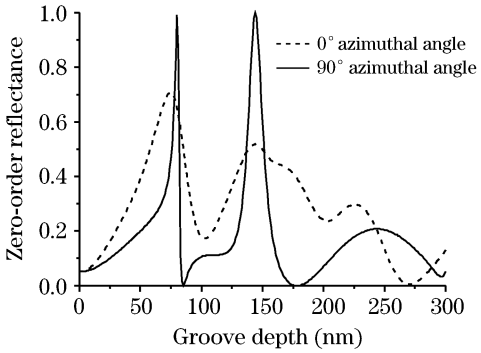

Fig. 4. Dependence of reflectance and groove depth of authenticating device. $\lambda = 440$ nm, $\phi = 0°$ (dashed curve); $\lambda = 582$ nm, $\phi = 90°$ (solid curve); $n_{\rm gH} = 2.35$, $n_{\rm gL} = 1.46$; $n_{\rm sub} = 1.46$; $\Lambda = 400$ nm; $f = 0.5$.

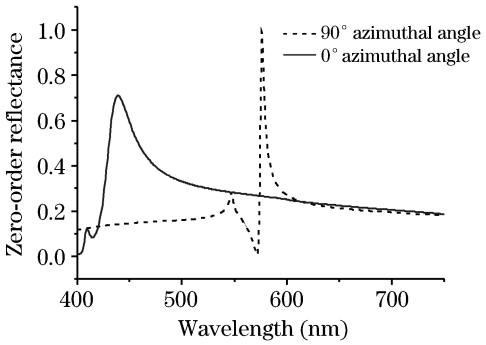

Fig. 5. Reflectance of single-layer GMRF. $\phi = 0°$ (the solid curve); $\phi = 90°$ (the dashed curve), $n_{\rm gH} = 2.35$, $n_{\rm gL} = 1.46$; $n_{\rm sub} = 1.46$; $\Lambda = 400$ nm; $f = 0.5$; $d = 75$ nm.

applications. The 149-nm groove depth is paid attention too, but it is too deep to be fabricated. So 75 nm is the optimum groove depth.

Figure 5 shows that when the azimuthal angles are 0° and 90°, the reflectance shapes are not symmetrical. Furthermore, the sideband is too high. The reflectance is more than 20% from 439 nm to 713 nm at the 0° azimuthal angle. The usual method of suppressing the reflectance sideband of the GMRF is the optimization of sub-waveguide thickness[1,12]. Here the method of using the layer with a low refractive index covered on the top of the grating structure is proposed. To avoid coping, one layer is usually covered on the top of the grating structures of an authenticating device. It is interesting to note that the thickness of this cover layer, with a low refractive index, has the effect of suppressing the reflectance sideband. Figure 6 gives this kind structure of double-layer GMRF.

As a common material with low refractive index, SiO_2 is chosen as the cover layer material by the anti-reflective thin-film design concept. To get a symmetrical shape and a low sideband of reflectance, the reflectance at two wavelengths is optimized. The first wavelength is 490 nm which has more reflectance (about 35%) for the 0° azimuthal angle. The second wavelength is 550 nm which has more reflectance (about 23%) for the 90° azimuthal angle. Figure 7 shows the dependence of the reflectance on the thickness of SiO_2 film at those two wavelengths. From the figure one can find that when the thickness of the cover layer is $75 - 95$ nm, the values of reflectance at two wavelengths are quite low ($< 10\%$). Therefore, 80 nm is chosen as the optimum thickness of cover layer. In fact, the depth of 80 nm is nearly quarter-wave thickness which is in compliance with anti-reflective (AR) requirements.

Figure 8 gives the reflectance of GMRF at 0° and 90° azimuthal angles when the thickness of cover layer film

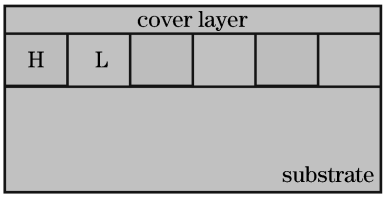

Fig. 6. Structure of double-layer GMRF. $n_{\rm cov} = 1.46$, $n_{\rm gH} = 2.35$, $n_{\rm gL} = 1.46$, $n_{\rm sub} = 1.46$, $\Lambda = 400$nm, $f = 0.5$, $d = 75$ nm.

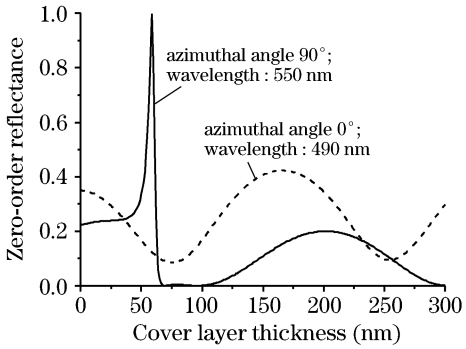

Fig. 7. Dependences of reflectance with the thickness of cover layer SiO_2 film. $\phi = 0°$ (the solid curve) at 490-nm wavelength; $\phi = 90°$ (the dashed curve) at 550-nm wavelength.

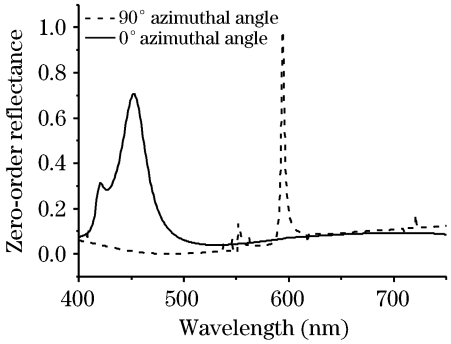

Fig. 8. Reflectance of authenticating device covered with 80-nm SiO_2 layer. $\phi = 0°$ (the solid curve); $\phi = 90°$ (the dashed curve), $n_{\rm gH} = 2.35$, $n_{\rm gL} = 1.46$; $n_{\rm sub} = 1.46$; $\Lambda = 400$ nm; $f = 0.5$; $d = 75$ nm.

is 80 nm. It is shown that the two reflectance responses are more symmetrical and the two resonant peaks (452 nm and 594 nm for the 0° and 90° azimuthal angles, respectively) are easily distinguished from each other. As shown in Fig. 8, the full-width at half-maximum (FWHM) is 30 nm at the 0° azimuthal angle and the FWHM is 4 nm at the 90° azimuthal angle. Therefore the FWHM, which is determined by the structures of the GMRF, is one parameter for further detection. Though the GMRF has not very good cut-off and peak shape, it appears two separate resonant peaks during the rotating in plane. So it has variable optical effect through azimuthal angles varying and can be applied to authentication labels. This kind structure of GMRF is difficult to be fabricated, especially for the filling of SiO_2 layer. But using the SOL-GEL fabrication technology of SiO_2 film and micro-contact printing method[13], it is possible to be fabricated. In fact, the complex fabrication technology is one requirement for authentication applications, because the device with simple technology is easy to be forged. GMRF and other devices with diffractive structures for authentication applicaitons are frequently refereed to as diffractive optically variable image device (DOVID). There is another kind of authentication devices usually called interference security image structure (ISIS)[14], such as some metal film filters or dielectric film filters which have variable optical effects. DOVID has higher anti-counterfeiting rank than ISIS in consideration of the counterfeiting difficulty[14].

In conclusion, a design for GMRF has been presented that can improve variable optical effects for authentication applications. When the azimuthal angle is 0°, the reflectance response has a resonant peak of 452 nm and a low sideband. After being rotated 90°, the device has a 594 nm resonant peak and a low sideband too.

The illumination angle is also investigated. It is found that as the illumination angle increases, the positions of the resonant peak at 0° and 90° azimuthal angles approaches and overlaps. 30° is the optimum angle for this variable optical effect. The reflectance response at the resonant wavelength is periodic oscillation with the groove depth. When groove depth is 75 nm, the reflectance response achieves its maximum for both the 0° and 90° azimuthal angles at the same time. To suppress the reflectance sideband, a method of controlling the thickness of a SiO_2 layer covering the top of the grating structure is used.

The authors would like to thank the reviewers and editors for their helpful suggestions and further help with English. This work was supported by the National Basic Research Program of China (No. 2007CB935303) and the Shanghai Committee of Science and Technology (No. 06DZ22016 and 07DZ22026). D. Zhang's e-mail address is dwzhang@siom.ac.cn.

References

1. Z. Hegedus and R. Netterfield, Appl. Opt. **39,** 1469 (2000).
2. R. Magnusson and S. S. Wang, Appl. Phys. Lett. **61,** 1022 (1992).
3. S. S. Wang and R. Magnusson, Opt. Lett. **19,** 919 (1994).
4. S. T. Thurman and G. M. Morris, Appl. Opt. **42,** 3225 (2003).
5. A. Mizutani, H. Kikuta, and K. Iwata, J. Opt. Soc. Am. A **19,** 1346 (2002).
6. D. Shin, Z. S. Liu, and R. Magnusson, Opt. Lett. **27,** 1288 (2002).
7. M. G. Moharam and T. K. Gaylord, J. Opt. Soc. Am. **72,** 1385 (1982).
8. D. W. Peters, S. A. Kemme, and G. R. Hadley, J. Opt. Soc. Am. A **21,** 981 (2004).
9. S. Boonruang, A. Greenwell, and M. G. Moharam, Appl. Opt. **45,** 5740 (2006).
10. M. T. Gale, K. Knop, and R. Morf, Proc. SPIE **1210,** 83 (1990).
11. M.-L. Wu and C.-L. Hsu, Opt. Lett. **32,** 1614 (2007).
12. S. S. Wang and R. Magnusson, Appl. Opt. **45,** 5740 (1995).
13. K. J. Lee and R. Magnusson, Integrated Photonics Research and Applications/Nanophotonics, Technical Digest (CD), NThA5 (2006).
14. V. R. Rudolf, Proc. SPIE **2406,** 268 (1995).